Local ordering in liquid metals probed by x-ray absorption spectroscopy

A. Di Cicco(1), F. Iesari(1), S. De Panfilis(2), A. Filipponi(3)

1. *Physics Division, School of Science and Technology, Università di Camerino, I-62032 Camerino (MC), Italy*
2. *Istituto Italiano di Tecnologia, Centre for Life Nanoscience–IIT@Sapienza, Viale Regina Elena 291, I-00161, Roma, Italy*
3. *Dipartimento di Scienze Fisiche e Chimiche, Università degli Studi dell'Aquila, I-67100 L'Aquila, Italy*

Overview

1. Introduction and motivations

2. Experiments and Techniques
   - X-ray Absorption Spectroscopy (XAS)
   - XAS measurements of liquids at extreme conditions
   - XAS structure refinement by Reverse Monte Carlo

3. Results
   - Bond-angle distribution in liquid metals
   - Local geometry probes
   - local geometry in close-packing liquids
   - icosahedral ordering and undercooling

Local ordering in simple liquids: undercooling and fivefold symmetry

- Metallic melts can be deeply undercooled below their freezing point [Langmuir(1943),Turnbull(1952)]
- Does the undercooling imply the existence of a more favourable local ordering in the liquid state?
- An icosahedral arrangement of 13 atoms is more stable than a fcc cluster [Frank (1952)] ...and also "A 13-atom LJ cluster embedded in a mean field LJ potential prefers the icosahedral arrangement" [Mossa et al.(2004)]
- Barrier to the transition between the metastable liquid and the thermodynamically stable solid

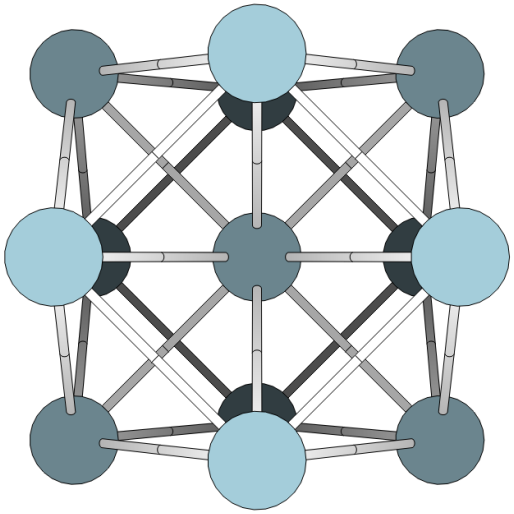
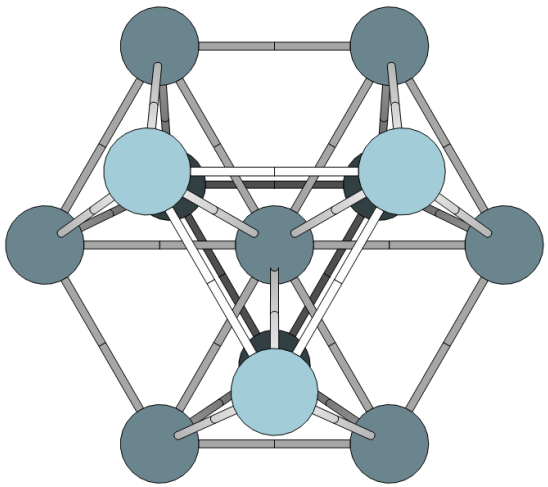
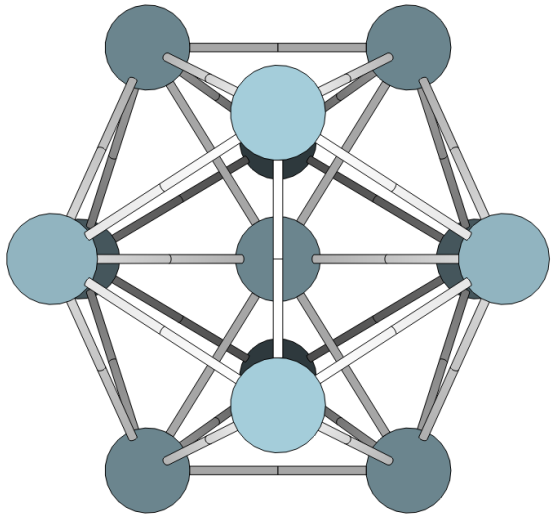

Local ordering in in simple liquids: some previous findings

- Signatures of five-fold local ordering have been previously found in several x-ray and neutron diffraction experiments (Reichert *et al.*, 2000; Schenk *et al.*, 2002; Kelton *et al.* 2007)
- Icosahedra, because of five-fold symmetry, are not consistent with crystal symmetry. Crystallization would hence require a complete rearrangement of the local order, which gives an explanation for undercooling.

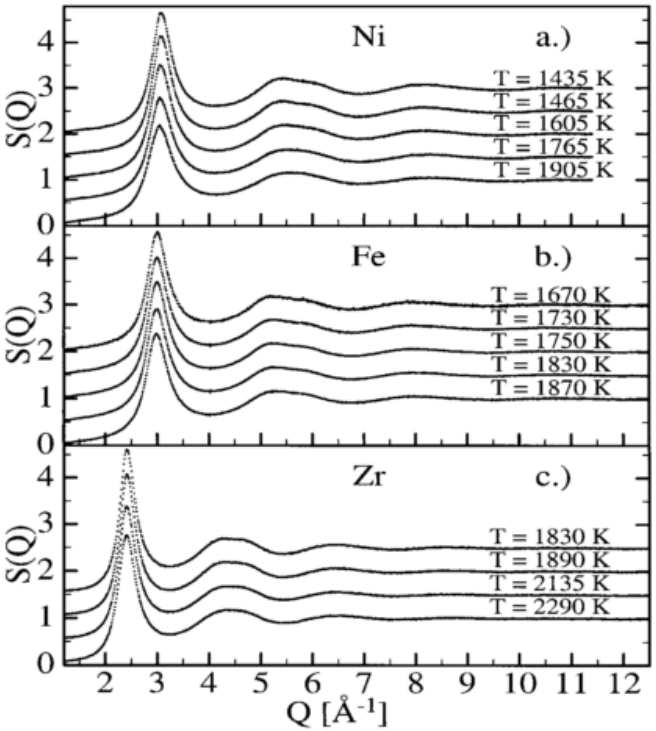

[T. Schenk, D. Holland-Moritz, V. Simonet, R. Bellissent and D. M. Herlach, Phys. Rev. Lett. **89**, 075507 (2002)]

Evidence of icosahedral short-range order in stable and deeply undercooled melts of pure metallic elements is obtained using the combination of electromagnetic levitation with neutron scattering (pair distribution). Icosahedral short-range ordering is shown to occur in the bulk metallic melt independently of the system investigated, increasing with the degree of undercooling.

X-ray absorption spectroscopy (XAS)

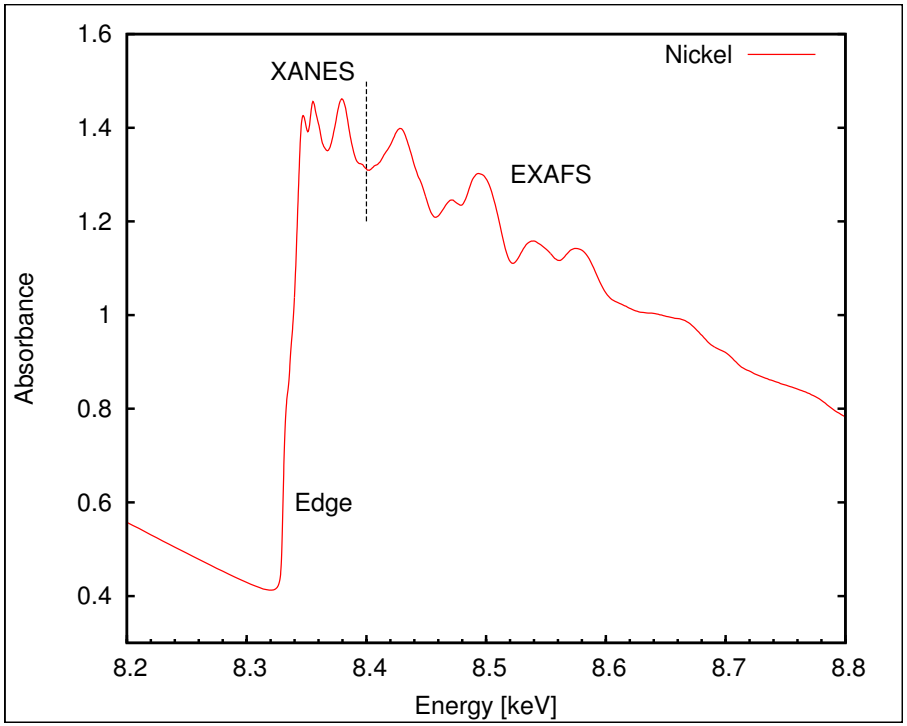

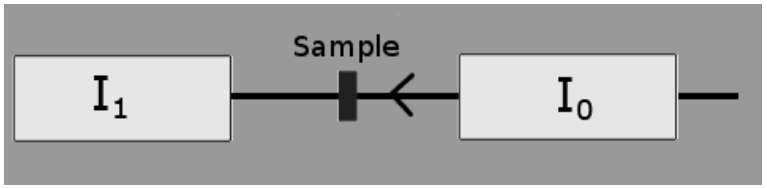

- absorbance: $\alpha(E) = \ln(I_0/I_1)$
- in an energy region beyond the core-edges, oscillations in the absorbance are present in condensed matter, referred as XAFS (X-ray absorption fine structure)

XAS and local geometry

XAS is extremely sensitive to short-range order (higher order distributions) and chemical selective, although being substantially unsensitive to long-range ordering. It is therefore especially suitable for highly disordered materials, amorphous and liquids and is strongly complementary with diffraction/scattering techniques.

XAS is also chemical selective.

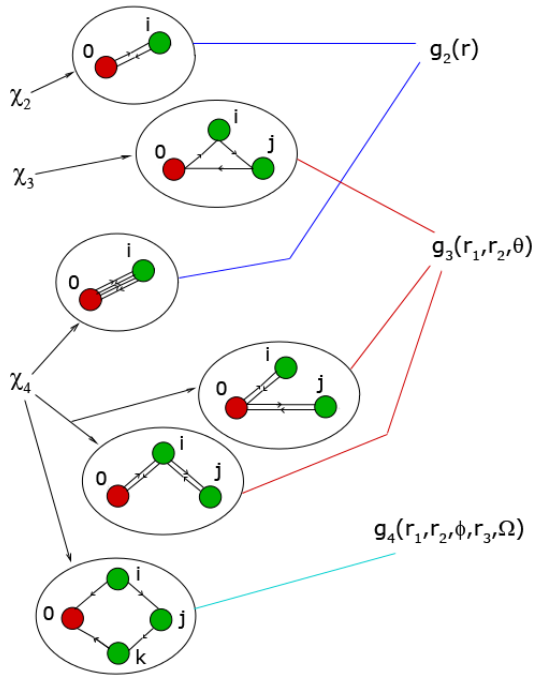

$$\langle\chi(k)\rangle = \int_0^\infty dr\, 4\pi r^2 \rho_0 g^{(2)}(r)\gamma^{(2)}(r,k) + \int dr_1 dr_2 d\phi\, 8\pi^2 r_1^2 r_2^2 \sin(\phi) \times \rho_0^2 g^{(3)}(r_1,r_2,\phi)\gamma^{(3)}(r_1,r_2,\phi,k) + \int dr_1 dr_2 d\phi dr_3 d\Omega\, 8\pi^2 r_1^2 r_2^2 r_3^2 \times \sin(\phi)\rho_0^3 g^{(4)}(r_1,r_2,\phi,r_3,\Omega)\gamma^{(4)}(r_1,r_2,\phi,r_3,\Omega,k) + \cdots \quad (1)$$

Combined XAS/XRD at high Temp./Pressures

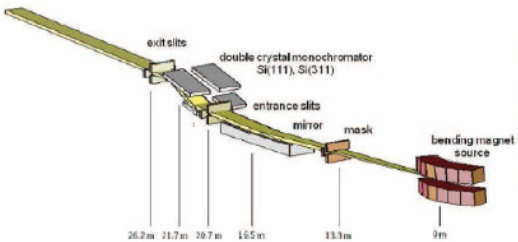

Figure 1. The basic optical concept of the XAFS beamline at ELETTRA. The mask define the size of the beam upstream the mirror. This one collimates the beam vertically before the double crystal monochromator in order to obtain the intrinsic energy resolution.

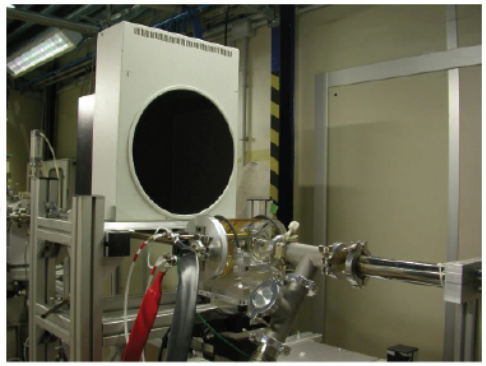

Figure 2. The high temperature L'Aquila-Camerino glass furnace for combined x-ray absorption and diffraction (custom version installed at XAFS@ELETTRA) and the vertical configuration for MAR image-plate detector.

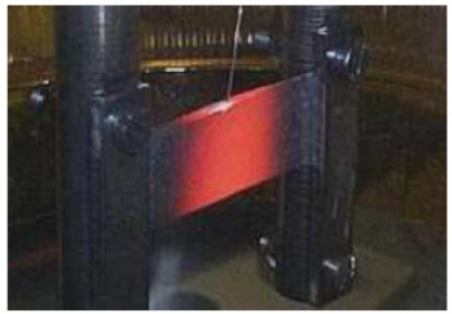

Nucl. Inst. & Methods in Phys. Res. B 93, 302 (1994)

- Wide temperature interval: 300÷2500 K
- Clean high-vacuum ($\sim 10^{-5}$ mbar) sample environment
- XAS/XRD measurements

Our high temperature XAS experiments began in Frascati (ADONE), late 80s and then suitable setups for the furnace were used at LURE (Orsay), ESRF and Elettra (since 2009). Simultaneous XRD/XAS spectra can be collected up to about 2500 K and more.

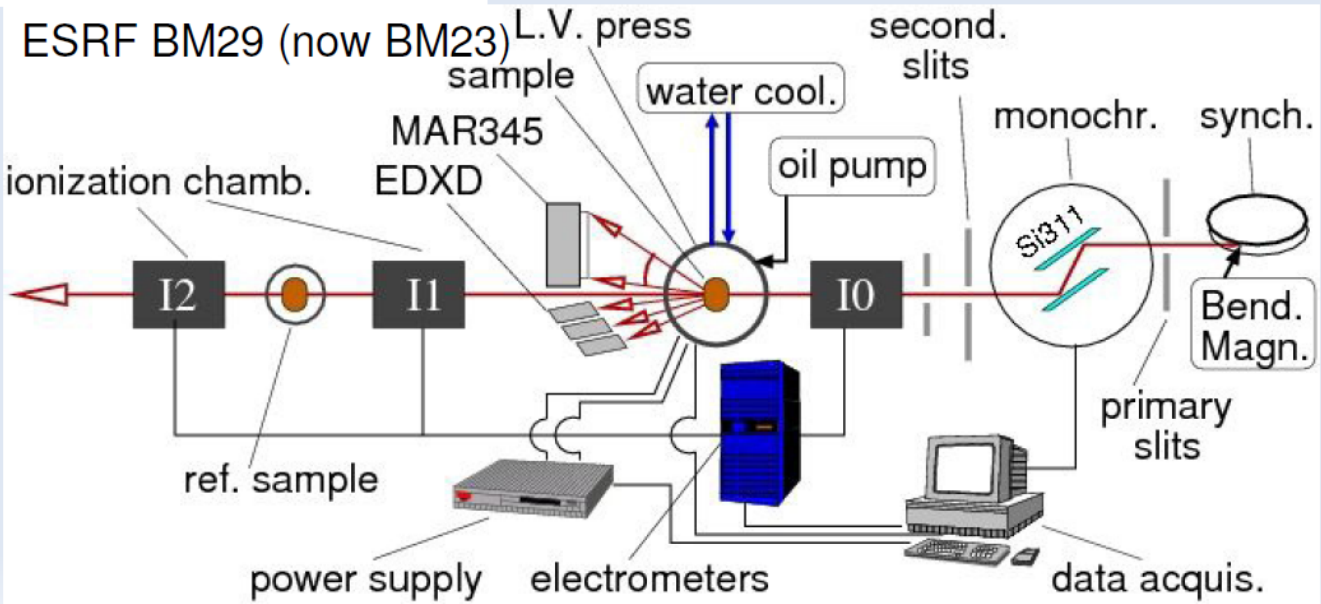

XAS for (undercooled) liquids

→ Samples for XAS in transmission mode: must be typically of micrometric thickness.
→ Thin liquid samples/droplets should be usually confined and/or maintained in position under extremely high temperatures, preserving uniform thickness and purity.

The sample is usually dispersed (b) into a "chemically inert" matrix, low x-ray absorbing and high-temperature resistant (like BN, C, Al_2O_3, ZrO_2). Micrometric powders of pure materials can be undercooled quite easily hundreds Celsius below the melting point.

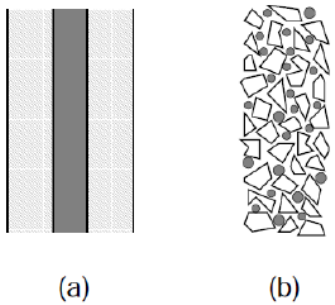

XAS: Easy access to liquid and undercooled states. Measuring the structure of metastable states

see for ex. "Is there icosahedral ordering in liquid and undercooled metals?", Phys. Rev. Letters 91, 135505 (2003), and Physical Review B 89, 060102 (2014).

Liquid nickel sample: submicrometric Ni droplets embedded in Al2O3.
Very good spectra obtained up to ~1800 K and exceptional undercooling (~350 K) observed.

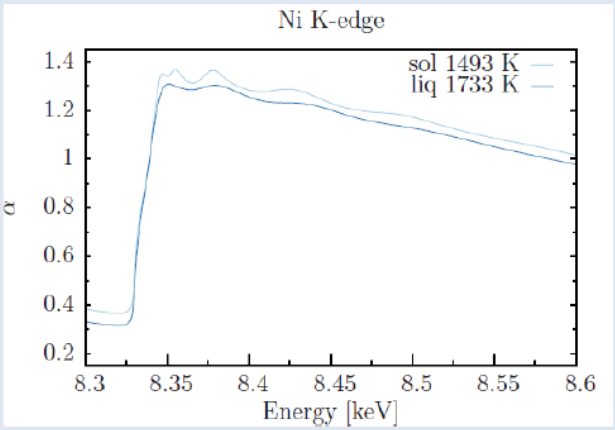

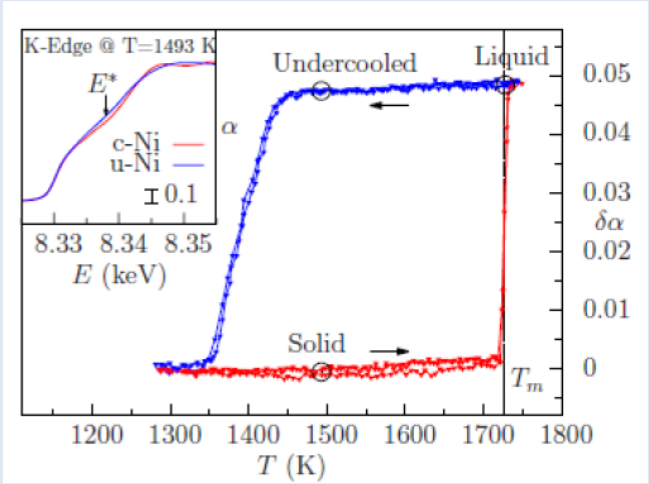

XAS structure refinement by Reverse Monte Carlo (RMC)

- In RMC, atom positions in a box are refined reproducing experimental data set(s). It is a variation of the standard Metropolis Monte Carlo (MMC), the agreement with experimental data plays the role of the energy potential.
- A new RMC data-analysis program for XAS has been designed (RMCXAS, based on the advanced GNXAS multiple-scattering XAS data-analysis program).

$$\chi^2 = \sum_{i=1}^{N_{XAS}} [k_i^n(\chi^E(k_i) - \chi^C(k_i))]^2/\sigma_i^2 + \\ + \sum_{j=1}^{N_g} [g^E(r_j) - g^C(r_j)]^2/\sigma_j^2$$

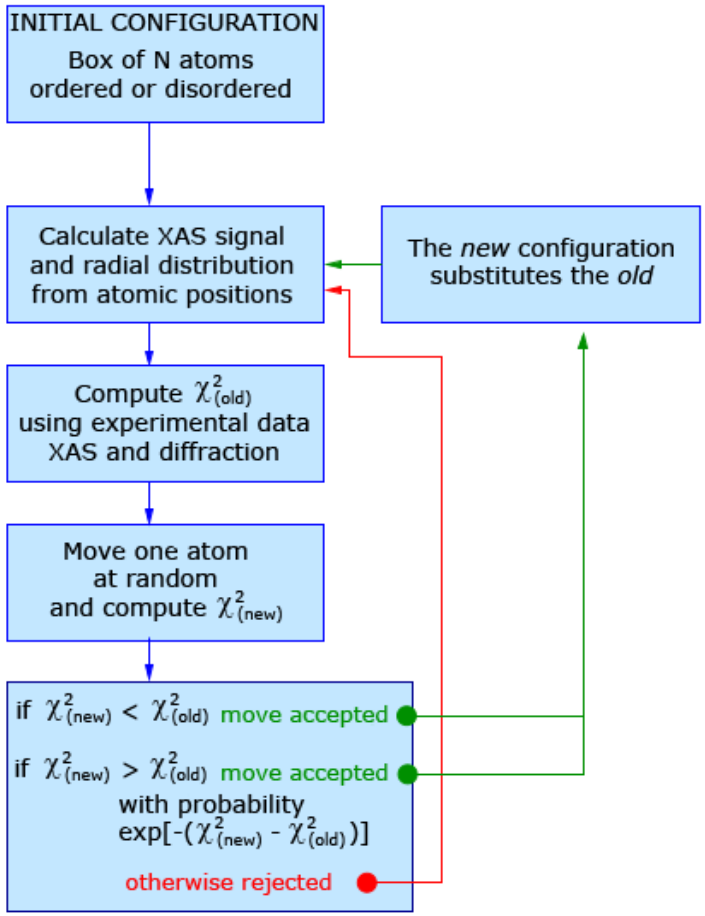

Unique insight on liquids by XAS

High-quality EXAFS spectra, differences among liquids at different temperatures

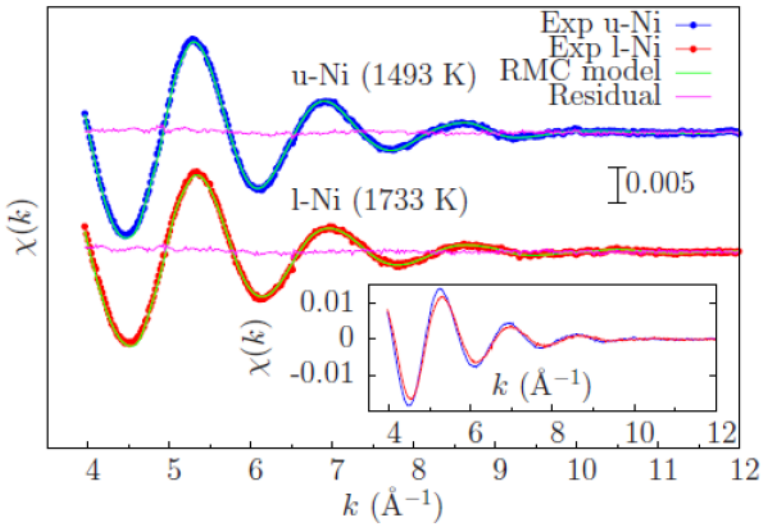

FIG. 2. Comparison of calculated (RMC simulation, green color on-line) and experimental EXAFS $\chi(k)$ signals for u-Ni (dots, red color on-line) and l-Ni (dots, blue color on-line) at 1493 K and 1733 K respectively. The flat residual confirms the quality of the refinement. The two experimental EXAFS signals are compared in the inset.

Refs: J. Phys. Condens. Matter 17 S135 (2005), Physical Review B 89, 060102 (2014)

→ Short-range of the liquid reconstructed by accurate multiple-scattering XAS data-analysis.

→ Pair and angular distributions obtained by Reverse Monte Carlo simulations using both XRD(ND) and XAS data

→ Type of local ordering (icosahedral or other) studied by various methods

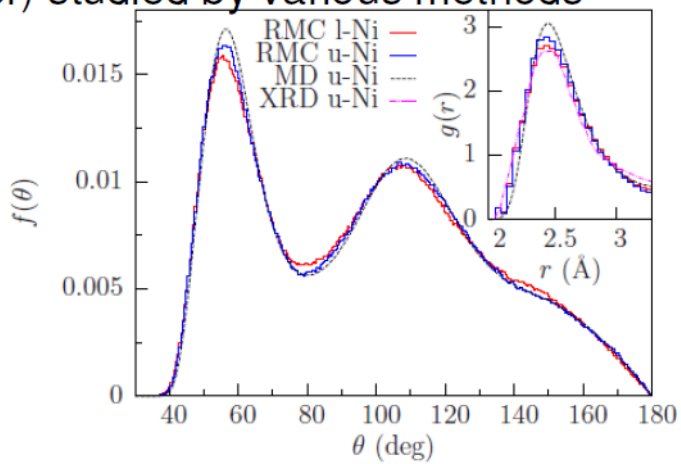

FIG. 3. Normalized bond angle distributions $f(\theta)$ calculated from MD (dashed) and RMC configurations for u-Ni (blue on-line) and l-Ni (red on-line). Inset: first peak of the pair distribution function $g(r)$ obtained by RMC-XAS for l-Ni (red color on-line) and u-Ni (blue color on-line), compared with MD results (dashed) and previous XRD data [19] (dot-dashed).

Bond angle distributions in different liquid metals

Typical close-packed liquid metal distribution, with peaks centered at 60° and 110° degrees and a minimum between.

These features are less pronounced for liquid Cd and. For liquids (Sn) containing open (mostly 4-fold) configuration a much broader distribution is obtained.

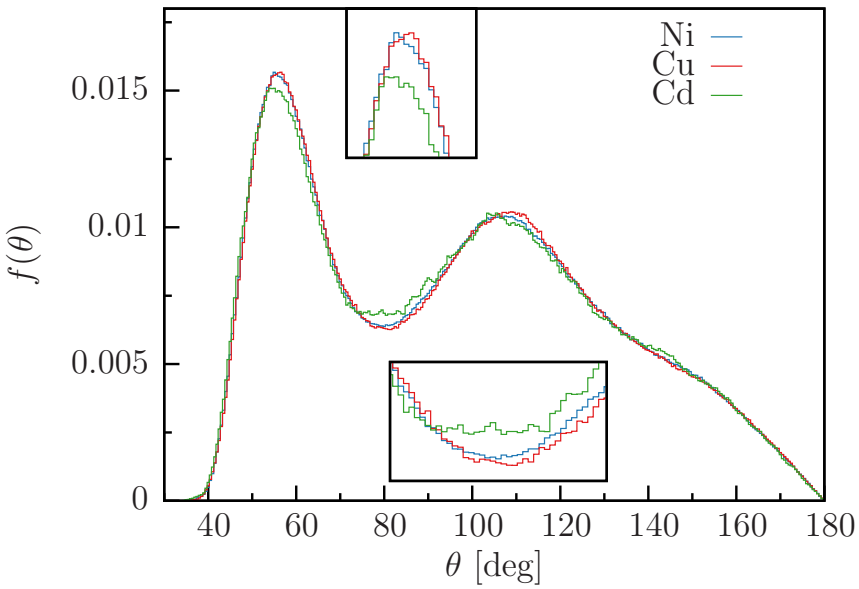

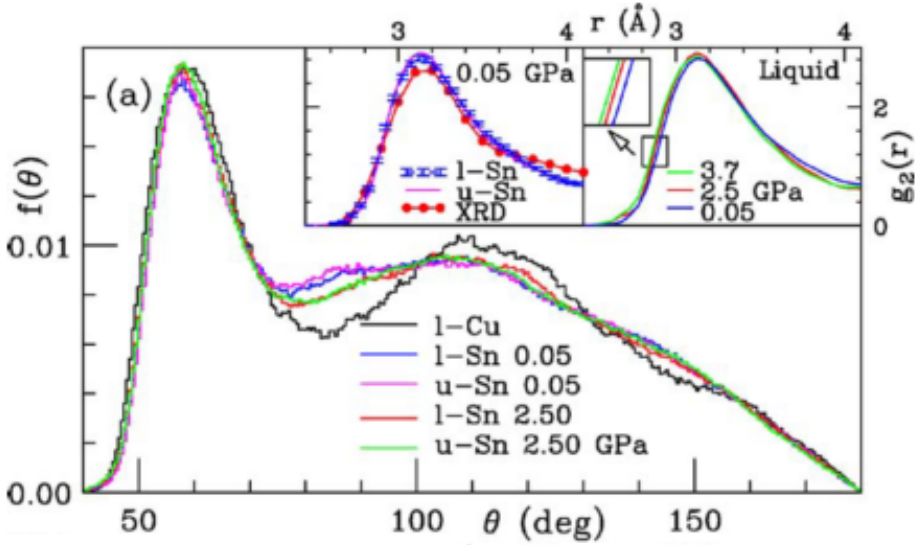

[Di Cicco, Trapananti *et al.*, Appl. Phys. Lett. **89**, 221912 (2006)]

Spherical harmonics invariant as a local geometry probe

Geometrical characterization of clusters through a set of spherical harmonics invariants (Steinhardt *et al.*, PRB **28**, 784 (1982)) calculated for each atom of the simulation at any equilibrium configuration.

$$Q_{lm} \equiv Y_{lm}(\theta(\vec{r}), \phi(\vec{r})) \qquad \bar{Q}_{lm} = \frac{1}{N_b} \sum_{\text{bonds}} Q_{lm}(\vec{r})$$

$$Q_l \equiv \left[\frac{1}{2l+1} \sum_{m=-l}^{l} | \bar{Q}_{lm} |^2 \right]^{1/2}$$

$$\hat{W}_l \equiv \frac{W_l}{\sum_{l=-m}^{m} \left[| \bar{Q}_{lm} |^2 \right]^{3/2}}$$

$$W_l \equiv \sum_{m_1+m_2+m_3=0} \begin{bmatrix} l & l & l \\ m_1 & m_2 & m_3 \end{bmatrix} \times \bar{Q}_{l_1 m_1} \bar{Q}_{l_2 m_2} \bar{Q}_{l_3 m_3}$$

	$\hat{W}_4$	$\hat{W}_6$	$\hat{W}_8$	$\hat{W}_{10}$
icos		−0.169 754		−0.093 967
fcc	−0.159 316	−0.013 161	+0.058 454	−0.090 128
hcp	+0.134 097	−0.012 442	+0.051 259	−0.079 854
bcc	+0.159 317	+0.013 161	−0.058 455	−0.090 130
sc	+0.159 317	+0.013 161	+0.058 455	+0.090 130

- fcc → $\hat{W}_6$=-0.013161
- icosahedron → $\hat{W}_6$=-0.169754 ($\hat{W}_l$=0 if l<6)

$\hat{W}_6$ distribution in close-packing liquids

Distribution of the $\hat{W}_6$ calculated from the RMC simulated equilibrium configurations $\Longrightarrow$ clusters defined by a cut-off distance (=2.8 Å) enclosing the first peak of the $g(r)$

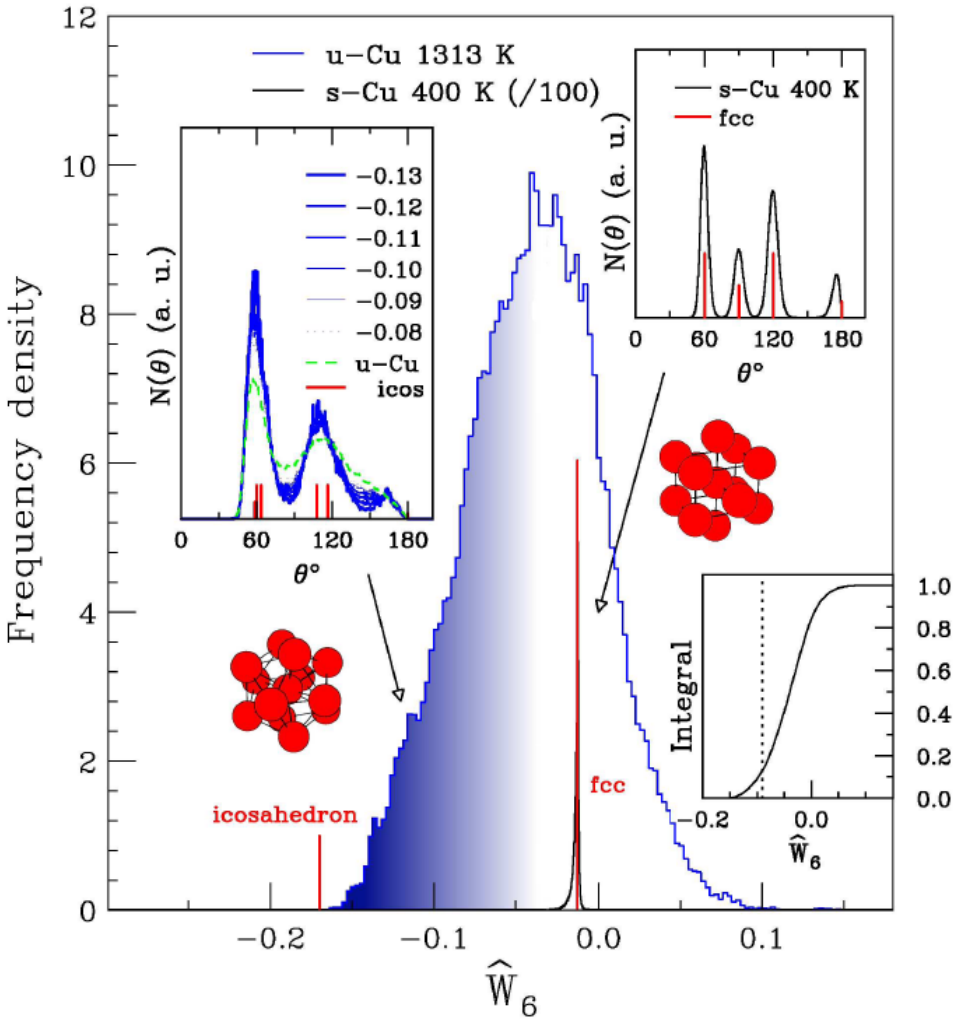

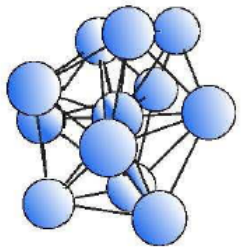

a cluster with $\hat{W}_6 \approx -0.13$

- Cut-off for nearly icosahedral clusters looking at the N(θ) distribution
- $N(\theta)$ of individual clusters having $\hat{W}_6$ < -0.09 resembles that of an icosahedron (broadening of $\approx 10°$)
- Fraction of nearly icosahedral configurations (about 10 %)

Common neighbours analysis

Each pair of nearest-neighbor atoms is classified by using a set of three indexes *jkl*: *j* is the number of nearest neighbors common to both atoms, *k* is the number of bonds between the common neighbors, and *l* is the number of bonds in the longest continuous chain formed by the *k* bonds between common neighbors.

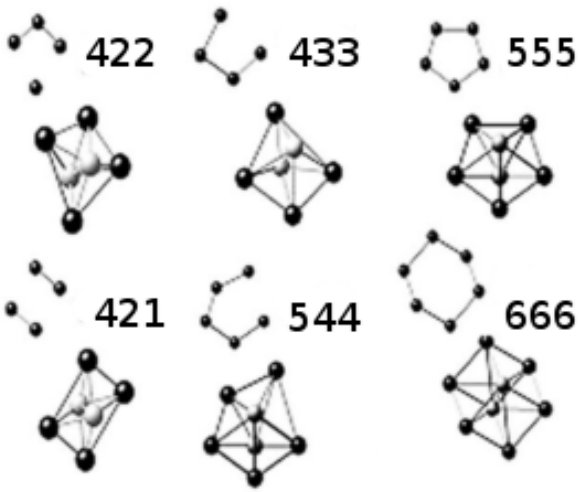

Different type of pairs are associated with different type of local order.
421 and 422 - fcc and hcp
433 and 544 - defective and distorted icosahedra
555 - icosahedra
666 - bcc

[Clarke and Jonsson, Phys. Rev. E **47**, 3975 (1993)]

CNA results on several liquids

	Ni	Cu	Cd
421 + 422	16%	15%	19%
433 + 544	40%	38%	34%
555	11%	10%	7%
666	3%	3%	2%

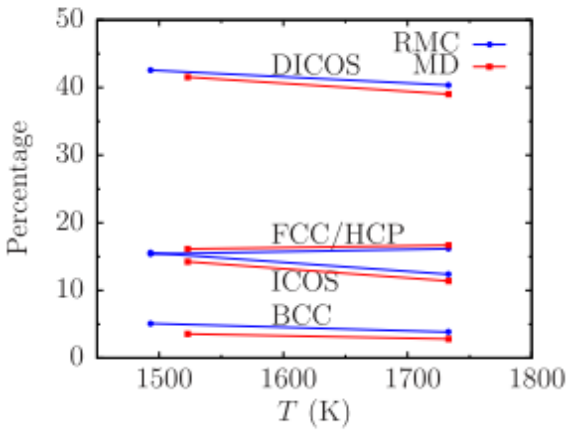

FIG. 4. (Color online) Percentage of nearest-neighbors pairs with given symmetry (CNA analysis of MD and RMC configurations). ICOS, icosahedral (555 pairs); DICOS, distorted icosahedral (544 and 433 pairs); BCC, bcc (666 pairs); and FCC/HCP, fcc and hcp (421 and 422 pairs).

Percentage of "perfect" local icosahedral structures (555) are in line with $\hat{W}_6$ results. A large fraction of 433 and 544 local configurations, corresponding to defective and highly-distorted icosahedra. fcc/hcp-like structures (666, 422, 421) are also found. Other disordered configurations are not included. Icosahedral ordering is found to increase in the undercooled liquid.

[Di Cicco, Iesari *et al.*, Phys. Rev. B **89**, 0601021(R) (2014)]
[Celino, Rosato *et al.*, Phys. Rev. B **75**, 174210 (2007)]